PB82-205881

Comparison of Telephotometer Measurements of Extinction Coefficients with Scattering and Absorption Coefficients

(U.S.) Environmental Sciences Research Lab.
Research Triangle Park, NC

1981

U.S. Department of Commerce
National Technical Information Service
NTIS.

TECHNICAL REPORT DATA
(Please read Instructions on the reverse before completing)

1. REPORT NO.	2.	3. RECIPIENT'S ACCESSION NO.
EPA-600/J-81-015	JOURNAL ARTICLE	

4. TITLE AND SUBTITLE	5. REPORT DATE
COMPARISON OF TELEPHOTOMETER MEASUREMENTS OF EXTINCTION COEFFICIENTS WITH SCATTERING AND ABSORPTION COEFFICIENTS	April 1982
	6. PERFORMING ORGANIZATION CODE
7. AUTHOR(S)	8. PERFORMING ORGANIZATION REPORT NO.
T.G. Dzubay and K.W. Clubb	
9. PERFORMING ORGANIZATION NAME AND ADDRESS Environmental Sciences Research Laboratory , RTP, NC Office of Research and Development U.S. Environmental Protection Agency Research Triangle Park, North Carolina 27711	10. PROGRAM ELEMENT NO. AAFA1D/01-1158 (FY-81) 11. CONTRACT/GRANT NO.
12. SPONSORING AGENCY NAME AND ADDRESS Environmental Sciences Research Laboratory, RTP, NC Office of Research and Development U.S. Environmental Protection Agency Research Triangle Park, North Carolina 27711	13. TYPE OF REPORT AND PERIOD COVERED 14. SPONSORING AGENCY CODE EPA/600/09

15. SUPPLEMENTARY NOTES
REFERENCE: Atmospheric Environment, 15(12):2617-2624, 1981.

16. ABSTRACT

During the summer of 1979, coefficients for light extinction in the atmosphere were calculated from measurements made with a telephotometer placed 251 m from a black target in Research Triangle Park, North Carolina. The results are well correlated (r = 0.92 to 0.96) with integrating nephelometer measurements of scattering coefficients and are highly correlated (r = 0.99) with daily averages of sums of scattering and absorption coefficients. The average sum of scattering and absorption coefficients accounts for about 90% of the average telephotometrically measured extinction coefficient; absorption by particles and nitrogen dioxide contributes 7% and 2%, respectively. From analysis of aerosol mass and composition, it is inferred that sulfate and its cations were the major cause of light extinction and haze at the measurement site.

17. KEY WORDS AND DOCUMENT ANALYSIS

a. DESCRIPTORS	b. IDENTIFIERS/OPEN ENDED TERMS	c. COSATI Field/Group

18. DISTRIBUTION STATEMENT	19. SECURITY CLASS (This Report)	21. NO. OF PAGES
RELEASE TO PUBLIC	UNCLASSIFIED	
	20. SECURITY CLASS (This page)	22. PRICE
	UNCLASSIFIED	

EPA Form 2220-1 (9-73)

PB82-205881

EPA-600/J-81-015
Journal Article

Reprinted from

ATMOSPHERIC ENVIRONMENT

Vol. 15, *No.* 12, *pp.* 2617–2624

COMPARISON OF TELEPHOTOMETER MEASUREMENTS OF EXTINCTION COEFFICIENTS WITH SCATTERING AND ABSORPTION COEFFICIENTS

T. G. DZUBAY and K. W. CLUBB

Environmental Sciences Research Laboratory, U.S. Environmental Protection Agency, Research Triangle Park, NC 27711, U.S.A.

REPRODUCED BY
NATIONAL TECHNICAL
INFORMATION SERVICE
U.S. DEPARTMENT OF COMMERCE
SPRINGFIELD, VA 22161

PERGAMON PRESS
NEW YORK · OXFORD · TORONTO · SYDNEY
PARIS · FRANKFURT
1981

Atmospheric Environment Vol. 15, No. 12, pp. 2617–2624, 1981
Printed in Great Britain.

0004-6981/81/122617-08 $02.00/0
Pergamon Press Ltd.

COMPARISON OF TELEPHOTOMETER MEASUREMENTS OF EXTINCTION COEFFICIENTS WITH SCATTERING AND ABSORPTION COEFFICIENTS

T. G. DZUBAY and K. W. CLUBB

Environmental Sciences Research Laboratory, U.S. Environmental Protection Agency, Research Triangle Park, NC 27711, U.S.A.

(*First received* 3 *November* 1980 *and in final form* 7 *May* 1981)

Abstract—During the summer of 1979, coefficients for light extinction in the atmosphere were calculated from measurements made with a telephotometer placed 251 m from a black target in Research Triangle Park, North Carolina. The results are well correlated ($r = 0.92$–0.96) with integrating nephelometer measurements of scattering coefficients and are highly correlated ($r = 0.99$) with daily arithmetic averages of sums of scattering and absorption coefficients. The average sum of scattering and absorption coefficients accounts for about 90% of the average telephotometrically measured extinction coefficient. Scattering by particles and scattering by air contribute 75 and 7% of the measured extinction coefficient; absorption by particles and absorption by nitrogen dioxide contribute 7 and 2%, respectively. From measurements of the aerosol mass and elemental composition, it is inferred that sulfate and its cations account for at least 54% of the mass of particles smaller than 2.5 μm in dia.

INTRODUCTION

Investigators have analysed airport visibility data obtained by the National Weather Service and noted a trend toward decreasing visibility in the United States between 1950 and 1974 (Trijonis and Yuan, 1978; Trijonis, 1979; Husar and Patterson, 1980). Although the trend is slight for urban sites in the East, it is pronounced for suburban and rural sites in the East and for sites in the Southwest. Dramatic decreases in summertime visibility occurred in the vicinity of North Carolina, Tennessee and Kentucky. Trijonis and Yuan (1978) used multiple regression calculations to show that particulate sulfate was a major factor in visibility degradation in the East. Husar and Patterson (1980) noted that the trend toward decreasing visibility in the East coincided with a trend toward increased coal consumption.

The human observer method, which provided the data used in detecting such trends, cannot be used if the location of the study does not offer suitably placed black targets viewable against the horizon sky. In the vicinity of our laboratory, the terrain is fairly flat and wooded, and lacks appropriate black targets. The same is true for the area around the Raleigh–Durham airport, located about 10 km to the southeast, (Trijonis and Yuan, 1978). Even without definitive measurements, the summertime visual air quality appears degraded by a conspicuous white haze; wooded canopies at distances much less than the visual range appear diminished in color and contrast.

Since measuring visual range or prevailing visibility was precluded by the character of our locale, we used the fact that the visual air quality can be characterized in terms of an extinction coefficient. For a spatially uniform aerosol under uniform illumination the extinction coefficient b_{ext} relates to contrast reduction by the expression

$$C(r) = C(0)\exp(-b_{ext}r) \tag{1}$$

where $C(r)$ is the contrast between an object and the sky when the object is viewed from distance r, and $C(0)$ is the contrast observed from zero distance (Koschmieder, 1924; Middleton, 1958; Tombach, 1978). The contrasts are related to object and sky brightness by the expressions

$$C(r) = [B_t(r) - B_s(r)]/B_s(r) \tag{2}$$

and

$$C(0) = [B_t(0) - B_s(0)]/B_s(0). \tag{3}$$

Here $B_s(r)$ and $B_t(r)$ are the apparent brightness of the sky s and target t when they are measured from a vantage point at distance r from the target; $B_s(0)$ and $B_t(0)$ are corresponding quantities measured at zero distance from the target.

Several investigators have examined the applicability of (1) and describe modifications for inhomogeneous atmospheres (Horvath, 1971; Malm, 1979; Middleton, 1958). If the targets are black and the observer can detect a minimum contrast of 0.02, then according to (1), visual range V and extinction coefficient are related by

$$V = 3.9/b_{ext}. \tag{4}$$

In the present work we use a telephotometer to measure the brightness of sky and target and deduce extinction coefficients using (1) (Coleman *et al.*, 1949; Middleton, 1958; Tombach and Allard, 1980). Because

our telephotometer had a spectral response similar to that of the human eye, the measured brightness quantity is luminance (Middleton, 1958) and will be referred to as such in the remaining text. If the telephotometer had a narrow band spectral response, the measured quantity would be radiance.

When using a telephotometer and a single target to determine extinction coefficients, it is necessary that $B_t(0)$ and $B_t(r)$ be determined simultaneously. Otherwise, diurnal changes in $B_t(0)$ due to changes in direction of solar illumination can lead to error in calculating b_{ext}. For example, Horvath (1971) has shown that the intrinsic contrast for buildings can change substantially during the day as the sun moves across the sky.

To avoid the inconvenience of having to make simultaneous measurements at distance r and at zero distance, we used a small black target located at distance $r = 251$ m. Because 251 m was small, we could assume that

$$B_s(r) = B_s(0).$$

Because the target was constructed so that its intrinsic luminance was essentially zero (i.e. $B_t(0) = 0$) it was unnecessary to monitor $B_t(0)$.

In determining extinction coefficients from the telephotometer data, it was necessary to correct for the fact that flare in the instrument's optical components produced a small but significant response to light from angles beyond that of its most sensitive region. The effect can be described algebraically by defining a parameter f by the equations

$$B'_t(r) = (1-f)B_t(r) + f\,B_s(r) \tag{5}$$

and

$$B'_s(r) = B_s(r) \tag{6}$$

where $B'_t(r)$ and $B'_s(r)$ are the telephotometer's responses to the actual target luminance $B_t(r)$ and sky luminance $B_s(r)$, respectively. We determine f by measuring the apparent luminance of the horizon sky and two similar targets at distances r_1 and r_2, which subtend equal angles. Using the preceding equations one can show that

$$(1-f)C(0) = -\left[1 - B'_t(r_1)/B_s\right]^{Z}\left[1 - B'_t(r_2)/B_s\right]^{1-Z} \tag{7}$$

and

$$C'(r) = (1-f)C(0)\exp(-b_{ext}r) \tag{8}$$

where

$$Z = r_2/(r_2 - r_1) \tag{9}$$

and

$$C'(r) = \left[B'_t(r) - B'_s(r)\right]/B'_s(r). \tag{10}$$

For the telephotometer data reported here, (7) was used to determine the quantity $C(0)(1-f)$, and (8) was used to determine the extinction coefficient.

In a second method, we determine extinction coefficient in terms of the following sum of components

$$b_{ext} = b_{sp} + b_{ap} + b_{sg} + b_{ag} \tag{11}$$

where b_{sp} and b_{ap} are the scattering and absorption coefficients for particulate matter, and b_{sg} and b_{ag} are the scattering and absorption coefficients for gas molecules (Waggoner and Charlson, 1976). We measured the scattering coefficient using an integrating nephelometer (Ahlquist and Charlson, 1967; Charlson *et al.*, 1969) and measured b_{ap} by a method involving transmission of light through filter-collected aerosol particles (Lin *et al.*, 1973; Weiss *et al.*, 1979). We deduced b_{ag} from nitrogen dioxide data (Charlson *et al.*, 1972; Mueller, private communication, 1980).

Below we report telephotometer measurements on flare and extinction coefficients and compare the latter with the sum of scattering and absorption coefficients. Our comparison is based upon 82 pairs of telephotometer and integrating nephelometer measurements made between 8 June and 3 August 1979. For twelve of the days, we analysed absorption coefficient, mass, and elemental composition of aerosol collected in a dichotomous sampler.

EXPERIMENTAL PROCEDURE

The sampling site was a grassy field surrounded by wooded areas in Research Triangle Park, N.C. There is a road beyond a patch of trees about 70 m to the west and a freeway about 600 m to the east. A telephotometer, an integrating nephelometer and an automated dichotomous sampler were operated in a small brick shelter at the west end of the field.

Light scattering coefficients were measured using a model 1561 integrating nephelometer manufactured by Meteorology Research, Inc., Altadena, CA*. Prior to our study this integrating nephelometer was modified and adjusted for improved sensitivity and stability by A. P. Waggoner, University of Washington, Seattle, WA. The device contained a Kodak Wratten 58 filter, which made its effective wavelength of response equal to 530 nm. Data were recorded using a strip chart recorder. The average outdoor temperature for the daytime measurement periods was 31 °C; the average temperature of the air stream at the integrating nephelometer's exhaust was 5 °C higher. This temperature rise was partly due to heating of air in the nephelometer by the instrument's lamp and electronic components. However, an air blower was located between the nephelometer chamber and the exhaust port where the temperature was measured. Thus, the actual temperature rise of the air in the nephelometer may have been somewhat less than 5 °C.

Each day the integrating nephelometer output was set at zero by purging the instrument with ambient air, filtered to make it particle free. At least twice weekly the instrument was span calibrated by filling it with dichlorodifluoromethane (F-12). The span calibration constant was deduced as follows: According to Penndorf (1957) the scattering coefficient for air is 14.3 Mm^{-1} (1 $Mm^{-1} = 10^{-6}\,m^{-1}$) for 530 nm wavelength light under standard conditions (T = 0 °C and P = 1013.25 mbar). According to Bodhaine (1979) the ratio of scattering coefficients for F-12 and air is 15.3. Thus, the scattering coefficient for F-12 at 530 nm and standard conditions

* Mention of commercial equipment or company names does not constitute endorsement by the U.S. Environmental Protection Agency.

is 219 Mm^{-1}. At our experimental site the average barometric pressure was 1002 mbar, and the average temperature at the exhaust of the integrating nephelometer was 36°C. Under such conditions the scattering coefficients at 530 nm wavelength are 191 Mm^{-1} and 12.5 Mm^{-1} for F-12 and air, respectively. Since our zero calibration procedure caused the air scattering coefficient (12.5 Mm^{-1}) to be subtracted from the total scattering coefficient, we used 179 Mm^{-1} for the F-12 span calibration constant. By using such a calibration constant, the integrating nephelometer should record b_{sp} at actual temperature and pressure conditions.

The automated dichotomous sampler was obtained from Beckman Instruments, Inc., Fullerton, CA, and it collected particles in 0–2.5 μm and 2.5 μm to about 15 μm dia. size ranges on 0.4 μm pore size Nuclepore filters (Nuclepore Corp., Pleasanton, CA). Total inlet flow rate was set at 16.7 ℓ min^{-1} (actual conditions) using a dry test meter. Sample durations were either 12 h with filter changes at 0630 and 1830, or 8 h with filter changes at 2300, 0700 and 1500 Eastern Standard time. The samples were analysed for mass by beta radiation attenuation in a device developed by Jaklevic *et al.* (1980). Elemental composition was determined using an energy dispersive X-ray fluorescence spectrometer developed by Jaklevic *et al.* (1976) and using procedures described by Dzubay and Rickel (1978) and Drane *et al.* (1980).

Time averaged values of the light absorption coefficient b_{ap} were measured by transmission of monochromatic light through filter-collected fine particles and through a Lambert scattering plate (Lin *et al.*, 1973). The geometrical arrangement of light source, sample, scattering plate and detector was identical to that of Lin *et al.* except that the deposit side of the sample was oriented toward the light source as illustrated by Weiss *et al.* (1979). A light emitting diode, having emission at 520 nm wavelength, was used as the light source, and transmitted light was detected using a photomultiplier tube. The absorption coefficient for the fine particle fraction was determined from the expression

$$I = I_0 \exp(-b_{ap} L) \tag{12}$$

where I_0 and I are the initial and final values of transmitted light intensity, and L is the ratio of air volume sampled to deposit area.

Values of b_{ext} were deduced from measurements using a model 2009 telephotometer obtained from Gamma Scientific, Inc., San Diego, CA. All measurements were made through a photopic filter having a peak transmissivity at 550 nm wavelength. The telephotometer's 2° aperture was used for all measurements. For quality assurance purposes, measurements were repeated using a 6° aperture. After each telephotometer measurement, relative humidity was measured outdoors using a sling psychrometer.

The telephotometer target was located 251 m from the telephotometer on the roof of a laboratory building to the northeast. The telephotometer–target line made a 4° angle with the horizontal plane. The target was a trapezoidal wooden box, 122 cm wide by 122 cm high by 122–183 cm deep [See Fig. 1(a)]. The open end of the box had two circular baffles of 61 and 76 cm dia. All interior surfaces of the box were painted matt black.

For each measurement, luminances were recorded for the target and for the sky 1° above the target. We did not calibrate the telephotometer in absolute units of luminance since only ratios of luminances are needed in (8) and (10). However, it is necessary that the zero level on the telephotometer be set correctly, and this was checked periodically during the experiment.

After completion of the measurements described above, two experiments were conducted to determine the flare parameter f. In the first, the target illustrated in Fig. 1(b) was located 251 m from the telephotometer, and a similar box which subtended the same solid angle was located collinearly at a distance of 47.6 m. Measurements were made of

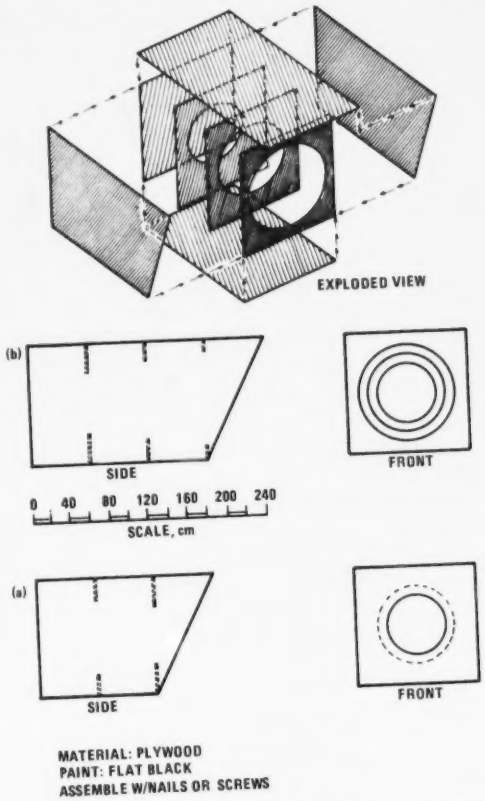

Fig. 1. Cross sectional and front views of telephotometer targets. An exploded view is also shown for target (b).

$B_t'(r_1)$, $B_t'(r_2)$, B_s'. In addition $B_t'(0)$ was measured with the telephotometer positioned at the target opening.

In the second experiment to determine flare, two targets were used also. One was the box shown in Fig. 1(b) located at a distance of 251 m toward the northeast; the second was a 5 cm dia. blackened tube located toward the north at distances ranging from 1 to 67 m. Luminance measurements pertaining to the box target and sky were used to determine b_{ext}; this value plus luminance measurements pertaining to the tube and sky were used in (8) to determine f for the tube.

RESULTS AND DISCUSSION

Flare measurements

Table 1 lists results of measurements of telephotometer flare. The results for the trapezoidal box target were deduced from (7). The value used for the intrinsic contrast was $C(0) = -0.9985 \pm 0.001$, which was determined from measurements with the telephotometer located at the box opening. According to Table 1, there is good agreement between results for both box and tube when their target sizes are similar. The flare parameter f decreases with increasing target size, but f did not reach zero for the target sizes considered.

Because we operated the telephotometer inside an enclosure which provided shade, we know that sun-

Table 1. Telephotometer flare measurements for box target shown in Fig. 1(b) and for 5 cm dia. tube target

Target	Target size	Flare parameter f 2′ Aperture	6′ Aperture
Box*	17′	0.0180 (0.0015)†	0.0215 (0.0013)‡
Tube	3.4′	0.029	0.59
Tube	6.9′	0.023	0.11
Tube	14′	0.020	0.027
Tube	35′	0.021	0.029
Tube	76′	0.017	0.021
Tube	150′	0.011	0.011
Tube	210′	0.008	0.008

* Angle based upon full 122 cm width of box.
† Standard deviation for nine measurements.
‡ Standard deviation for eight measurements.

light scattered by the lens hood was not the cause of the flare. Moreover, we are not misinterpreting a nonzero intrinsic target brightness as flare. Measurements made close to the box target indicate that when the sun is not shining directly into the box, the ratio $B_i'(0)/B_s$ is less than 0.005, which is small compared to $f = 0.018$ for the target at a distance of 251 m. Also, the tube results do not change appreciably when a shadow is cast on the tube opening, which indicates that its intrinsic brightness is not a major factor. However, placing a large black object behind the tube target led to a substantial reduction in instrument response. Thus, we conclude that the flare is caused by light from beyond the target, which reaches the sensor in the telephotometer. The problem of flare is not unique to the instrument used in this experiment. We tested another commercially available telephotometer and found that its flare was larger than the flare in our instrument.

Comparison of scattering, absorption and extinction coefficients

The results of the measurements are shown in Tables 2 and 3 and Figs 2 and 3. The telephotometer measurements shown were made using the instrument's 2′ aperture and using the target shown in Fig. 1(a). Values of b_{ext} were calculated using the flare value $f = 0.018$ in (8). To avoid biasing the results, meteorological conditions such as clouds and rain were not considered in setting our measurement schedule. Each scattering coefficient was obtained by averaging the integrating nephelometer results over a 15-min time interval bracketing a telephotometer measurement. Most of the paired telephotometer and integrating nephelometer measurements were made between 0830 and 1600 h Eastern Standard time. The light absorption coefficient measurements represent 8- and 12-h daily averages for particles in the 0–2.5 μm dia. range.

Figure 2 is a plot of all 82 pairs of telephotometer and integrating nephelometer measurements. To each value of b_{sp} the air scattering value $b_{sg} = 12.5\ Mm^{-1}$ is added. Table 2 shows linear least squares regression parameters for the paired data in various ranges of relative humidity.

In Fig. 2, the two highest relative humidities (90 and 86%) are plotted as solid circles. For one of those points, the telephotometer result is substantially larger than the integrating nephelometer result. This may be an instrumental artifact associated with the air tem-

Table 2. A comparison of paired telephotometer results for b_{ext} and integrating nephelometer results for $b_{sp} + b_{sg}$ in various ranges of relative humidity

r.h. Range %	N*	r†	A‡ Mm^{-1}	B‡	Error of estimate§ Mm^{-1}	Average b_{ext} Mm^{-1}	Ratio‖
0–90	82	0.92	−2 (18)	1.27 (0.12)	43	163	1.25
0–85	80	0.94	1 (15)	1.22 (0.10)	36	158	1.23
0–80	78	0.94	0 (15)	1.22 (0.10)	36	154	1.22
0–70	62	0.94	−3 (17)	1.22 (0.11)	36	149	1.20
0–65	52	0.95	−9 (17)	1.21 (0.11)	33	148	1.15
0–60	41	0.96	−12 (19)	1.23 (0.12)	34	149	1.14

* Number of measurements.
† Correlation coefficient.
‡ Intercept and slope from the linear regression $b_{ext} = A + B\ (b_{sp} + b_{sg})$. The values in parentheses represent half widths of the 95% confidence intervals.
§ $\sqrt{\Sigma[b_{ext}(i) - \bar{b}_{ext}(i)]^2/(N-2)}$, where $\bar{b}_{ext}$ is calculated in the linear regression.
‖ Ratio of average value of b_{ext} to average value of $b_{sp} + b_{sg}$.

Table 3. Comparison of average extinction coefficient with average sum of components for data in different ranges of relative humidity

Parameter	Method	Coefficient, Mm^{-1} r.h. $\leq 65\%$*	r.h. $\leq 85\%$†
b_{sp}	Integrating nephelometer	126	126
b_{sg}	From literature	12	12
b_{ap}	Light transmission	11	12
b_{ag}	NO_2 concentration	3	3
b_{ext}	Equation (11)	152‡	153‡
b_{ext}	Telephotometer	163	171

* Arithmetic averages based upon 10 measurement days.
† Arithmetic averages based upon 12 measurement days.
‡ Sum of the above four values.

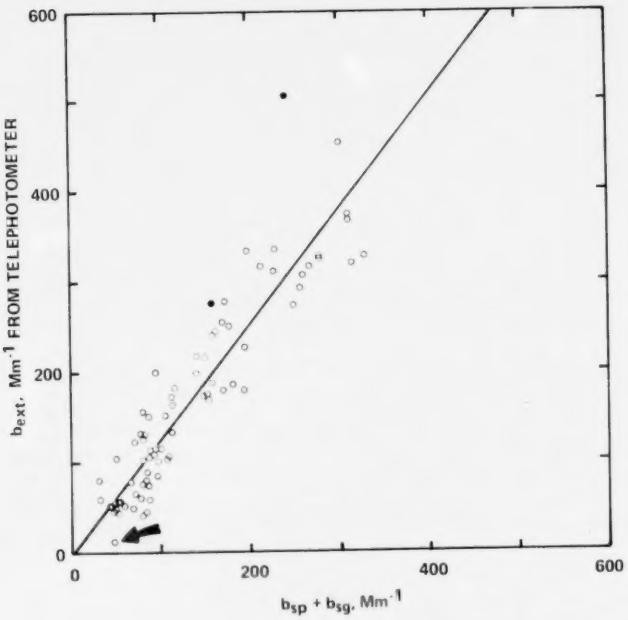

Fig. 2. Plot of extinction coefficients vs sums of scattering coefficients. The solid circles pertain to relative humidities above 85%; the open circles pertain to lower relative humidities. See text for discussion of datum indicated by arrow.

perature rise in the nephelometer described above. Any temperature rise would reduce the relative humidity, which would cause a reduction in both particle size and scattering coefficient for hygroscopic aerosol. Covert *et al.* (1972) demonstrated that ambient aerosol is hygroscopic and that the scattering coefficient rises steeply as the relative humidity is raised above 70–80%. As a further indication of the effects of relative humidity, Table 2 shows that as relative humidity is restricted to lower values, the ratios of telephotometer to integrating nephelometer values decrease, and the correlation coefficients increase.

Depending on the relative humidity (r.h.) interval, the correlation coefficients in Table 2 range from 0.92 to 0.96. In a previous comparison of a telephotometer and an integrating nephelometer operated near Seattle, Washington, Cwalinski *et al.* (1975) obtained correlation coefficients of 0.79, 0.83 and 0.74 for relative humidity in the ranges 0–65%, 0–80% and 0–90%, respectively. In that study, Cwalinski *et al.* used both natural targets and black box targets; no corrections were made for telephotometer flare or intrinsic target brightness.

In the comparisons made in Fig. 2 and Table 2, absorption coefficients were not included because their 8 to 12 h averaging times were not compatible with those of the telephotometer and integrating nephelometer. However, in Table 3 and Fig. 3 we do include absorption coefficients in comparisons of time-averaged coefficients. Data in Table 3 represent multi-

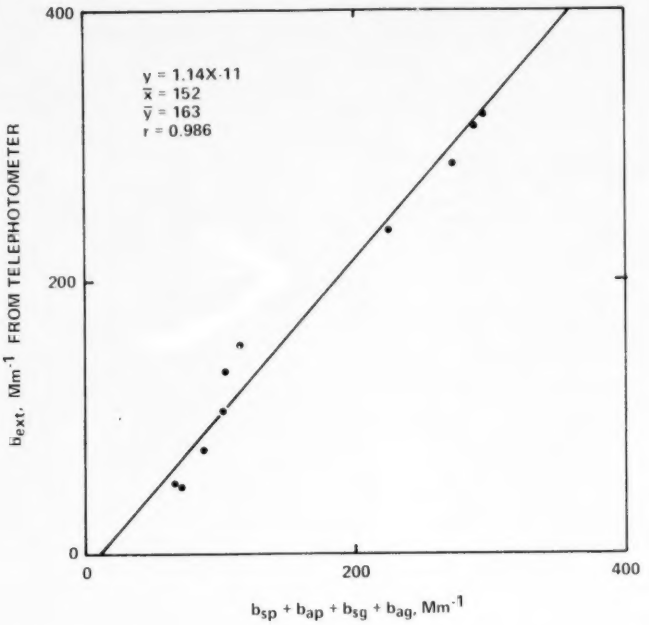

Fig. 3. Plot of daily averages of extinction coefficient vs daily averages of sums of scattering and absorption coefficients.

day arithmetic averages of scattering absorption, and extinction coefficients in two humidity ranges. For relative humidities below 85%, the averages are based upon 12 days on which all indicated parameters were measured. When the relative humidity was limited to 65% and below, only 10 days could be included. The data on b_{ag} were deduced from NO_2 measurements made at EPRI-SURE (Electric Power Research Institute—Sulfate Regional Experiment) site number 08 located 1 km to the east of our site (Perhac, 1978; Mueller, personal communication, 1980). For both humidity ranges an average nitrogen dioxide concentration of 6 ppb was obtained for time periods corresponding to the telephotometer measurements. The absorption coefficients were deduced using a conversion factor of $0.46\,Mm^{-1}\,ppb^{-1}$ for 530 nm wavelength light (Dixon, 1940).

Figure 3 is a plot of daily arithmetic averages of extinction coefficients derived from telephotometer measurements vs daily averages of sums of scattering and absorption coefficients. Only data for relative humidities below 65% are included. The intercept and slope for the linear regression are $-11\,Mm^{-1}$ and 1.14, respectively; their 95% confidence intervals have half widths of $27\,Mm^{-1}$ and 0.16. Thus, the intercept and slope are not significantly different from 0 and 1, respectively. The correlation coefficient is 0.986, and the error of extimate is $18\,Mm^{-1}$. The corresponding values in Table 2 are 0.95 and $33\,Mm^{-1}$. The relationship in Fig. 3 is more precise than that of Table 2, not only because absorption is included, but also because random error is reduced by averaging.

From Table 3, we conclude that scattering by particles accounts for about 75% of the extinction coefficient, and scattering by air accounts for 7%. Light absorption by particles accounts for about 7%—a value similar to those found in other rural areas but much smaller than those found in certain urban areas (Weiss *et al.*, 1979). Absorption by NO_2 accounts for less than 2%—a value much lower than those found in a previous study in Los Angeles, California (Charlson *et al.*, 1972). The average extinction coefficient measured by telephotometer exceeds the average sum of scattering and extinction coefficients in Table 3 by 7–11%. The difference may be due to systematic errors, which are discussed below.

Sources of error

Several sources of systematic error and random error can affect the comparisons. We have already discussed how relative humidity reduction in the integrating nephelometer can decrease the scattering coefficient. Angular truncation in the integrating nephelometer can also contribute a small systematic error (Ensor and Waggoner, 1970). Such an error results from a small angular region within the integrating nephelometer where forward scattered light is not collected. According to Ensor and Waggoner this can cause the response to be too low by about 3–4% for a typical Junge distribution of particles $< 10\,\mu m$. Another small source of systematic error is the slight difference between the telephotometer's and integrat-

ing nephelometer's wavelengths of response. The former has a broad response peaked at 550 nm; the latter has a narrow response at 530 nm. A large systematic error was avoided by making the flare correction. If we had neglected to do so, then our telephotometer data would have had a positive bias of 72 Mm^{-1}. If the value for flare is not constant, then random error will appear.

The "error of estimate" presented in Table 2 is an indication of random error. The values for the telephotometer vs integrating nephelometer comparison are about 35 Mm^{-1}. Part of this may be due to zero drift in the integrating nephelometer, which was about 20 Mm^{-1}. The telephotometer precision of 21 Mm^{-1} was estimated from 128 paired measurements using the instrument's 6′ and 2′ apertures. Some of this random error may be due to a temperature dependent zero signal drift affecting the 2′ data. The 2′ aperture would be much more affected by any offset, because it collects only 10% as much light as does the 6′ aperture. Actual fluctuations in the sky brightness and extinction coefficients would also introduce random error.

Error in telephotometer measurements of b_{ext} can also result from nonuniform illumination. A cloud casting a shadow over the telephotometer and target may cause the measured value to be too low. Conversely, a dark cloud which reduces the sky brightness behind the target may cause the measured value to be too large. One of our measurements was made when it was raining heavily at our site, but not at the airport 10 km to the east. The measurement made during these nonuniform conditions is identified by an arrow in Fig. 2. Not surprisingly, the telephotometer result deviates from the regression line.

Aerosol mass and composition

Calculations presented by Willeke and Brockmann (1977) indicate that mass in particles in the 0.1–1 μm dia. range is much more effective in scattering light than mass in particles larger than 3 μm. For our measurements the mass concentration (arithmetic average for days when the relative humidity was less than 65%) was 29 $\mu g\,m^{-3}$ and 18 $\mu g\,m^{-3}$ for particles in the 0–2.5 μm and 2.5–15 μm dia. ranges, respectively. From the plots made by Willeke and Brockmann (1977) we estimate that mass in the fine fraction is responsible for at least 95% of the light scattering, and mass in the coarse fraction is responsible for less than 5%. Using data from Tables 3 and 4, we find that the ratio of fine particle mass concentration to scattering coefficient is 0.23 $g\,m^{-2}$. This value is below the range 0.32 $\pm$ 0.02 $g\,m^{-2}$ found by Waggoner and Weiss (1980) for the aerosol in five areas in the western part of the United States. Our value may be lower for at least two reasons. One is that the air in our integrating nephelometer was heated to a lesser extent than was the case in the work done by Waggoner and Weiss. A second is that slight differences in the aerosol size distribution can affect the ratio significantly.

Since mass in the fine fraction is responsible for most of the extinction coefficient that we measured, it is useful to examine the composition. Table 4 shows average mass and elemental composition for particles in the 0–2.5 μm diameter range. Sulfur is one of the most abundant species. Measurements made at our site during the summers of 1977 and 1978 indicated that the sulfur occurred as a mixture of ammonium sulfate and sulfuric acid (Stevens *et al.*, 1978; Dzubay *et al.*, 1979). If the sulfur in the present experiment were in the form of ammonium sulfate, the latter would account for 54% of the mass in the fine fraction. If the sulfur occurred as sulfuric acid plus its associated water, then an even larger fraction would be accounted for.

Table 4. Average composition of aerosol particles in the fine (0–2.5 μm dia.) fraction*

Parameter	Concentration $\mu g\,m^{-3}$	Parameter	Concentration $\mu g\,m^{-3}$
Mass	29		
Al	< 0.1	Fe	0.1
Si	< 0.4	Cu	0.011
S	3.8	Zn	0.024
K	0.08	Br	0.020
Ca	0.05	Pb	0.21

* Averages (arithmetic) are based upon the same 10 days having relative humidity below 65% used to compute averages shown in Table 3.

CONCLUSIONS

This work demonstrates that it is possible to make accurate measurements of light extinction coefficients in the atmosphere by using a telephotometer and a black target located at a distance of about 250 m. However, when the target is so close, optical flare is an important parameter that must be measured and included in the calculations of extinction coefficients. The telephotometer results are well correlated ($r = 0.92$ to 0.96) with integrating nephelometer measurements and are highly correlated ($r = 0.99$) with daily averages of sums of scattering and absorption coefficients. Such results pertain to extinction coefficients which ranged from 50 to 500 Mm^{-1}. For pristine areas having smaller extinction coefficients, the telephotometer target would need to be larger and more distant if comparable results were to be obtained.

The average sum of scattering and absorption coefficients accounts for [illegible] 93% of the average telephotometrically measured extinction coefficient. Part of the small difference may be caused by loss of moisture on particles due to a slight warming in the integrating nephelometer used to measure scattering coefficients. Differences in spectral responses of the telephotometer and integrating nephelometer may also contribute to the difference between results.

Although the amount of random error was not large, we feel that steps can be taken in future experiments to reduce it. One would be to check the telephotometer zero before each measurement. A second would be to

make repetitive telephotometer measurements that can be averaged over 10 or 15 min periods. A third would be to make frequent zero checks on the integrating nephelometer. Waggoner (1980) has developed an automatic system for performing zero checks every 15 min. Furthermore, in future comparisons of telephotometer and nephelometer, both instruments should be equipped with optical filters that make their spectral responses identical.

A disadvantage of our telephotometer method is that it is labor intensive. Although this defect could be corrected by using an automated instrument, we feel that it is more important to use a telephotometer that has a minimal amount of optical flare.

From measurements of the aerosol mass and elemental composition we infer that sulfate and its associated cations account for at least 54% of the mass of particles smaller than 2.5 μm in dia.

Acknowledgements—We thank A. P. Waggoner for valuable discussions and advice and R. K. Stevens for his support and encouragement. We thank J. Adcock, W. J. Courtney, B. Mullen, C. Owen and C. Pressley for analysis of aerosol samples. We thank P. K. Mueller for providing EPRI-SURE data on nitrogen dioxide. We thank R. Barbour for typing this manuscript.

REFERENCES

Ahlquist N. C. and Charlson R. J. (1967) A new instrument for evaluating the visual quality of air. *J. Air Pollut. Control Ass.* **17**, 467–469.

Bodhaine B. A. (1979) Measurement of the Rayleigh scattering properties of some gases with a nephelometer. *Appl. Opt.* **18**, 121–125.

Charlson R. J., Ahlquist N. C., Selvidge H. and MacCready P. B. (1969) *J. Air Pollut. Control Ass.* **19**, 937–942.

Charlson R. J., Covert D. S., Tokiwa Y. and Mueller P. K. (1972) Multiwavelength nephelometer measurements in Los Angeles smog aerosol. *J. Colloid Interface Sci.* **39**, 260–265.

Coleman H. S., Morris F. J., Rosenberger H. E. and Walker M. J. (1949) A photoelectric method of measuring the atmospheric attenuation of brightness contrast along a horizontal path for the visible region of the spectrum. *J. opt. Soc. Am.* **39**, 515–521.

Covert D. S., Charlson R. J. and Ahlquist N. C. (1972) A study of the relationship of chemical composition and humidity to light scattering by aerosols. *J. appl. Met.* **11**, 968–976.

Cwalinski R., Lansinger J. M. and Tank W. G. (1975) Field testing and evaluation of methods for measuring visibility. U.S. Environmental Protection Agency, Report EPA-650/2-75-039, Research Triangle Park, NC.

Dixon J. K. (1940) The absorption coefficient of nitrogen dioxide in the visible spectrum. *J. Chem. Phys.* **8**, 157–160.

Drane E. A., Rickel D. G., Courtney W. J. and Dzubay T. G. (1980) Computer code for analyzing X-ray fluorescence spectra for airborne particulate matter. In *Advances in X-ray Analysis*. (Edited by J. R. Rhodes), Vol. 23, pp. 149–156. Plenum, New York, NY, U.S.A.

Dzubay T. G. and Rickel D. G. (1978) X-ray fluorescence analysis of filter collected aerosol particles. In *Electron Microscopy and X-ray Applications*. (Edited by P. A. Russell and A. E. Hutchings), pp. 3–20. Ann Arbor Science, Ann Arbor, MI.

Dzubay T. G., Snyder G. K., Reutter D. J. and Stevens R. K. (1979) Aerosol acidity determination of reaction with ^{14}C labelled amine. *Atmospheric Environment* **13**, 1209–1212.

Ensor D. S. and Waggoner A. P. (1970) Angular truncation error in the integrating nephelometer. *Atmospheric Environment* **4**, 481–487.

Horvath H. (1971) On the applicability of the Koschmieder visibility formula. *Atmospheric Environment* **5**, 177–184.

Horvath H. and Presle G. (1978) Determination of atmospheric extinction coefficient by measurement of distant objects. *Appl. Optics* **17**, 1303–1304.

Horvath H. and Noll K. E. (1969) The relationship between atmospheric light scattering coefficient and visibility. *Atmospheric Environment* **3**, 543–550.

Husar R. B. and Patterson D. E. (1980) Regional scale air pollution: sources and effects. *Ann. N.Y. Acad. Sci.* **338**, 399–417.

Jaklevic J. M., Gatti R. C., Goulding F. S. and Loo B. W. (1980) Beta gauge instrumentation for the measurement of aerosol mass. U.S. Environmental Protection Agency, Report EPA-600/7-80-081, Research Triangle Park, NC 27711, U.S.A.

Jaklevic J. M., Landis D. A. and Goulding F. S. (1976) Energy dispersive X-ray fluorescence spectrometry using pulsed X-ray excitation. In *Advances in X-Ray Analysis*. (Edited by R. W. Gould, C. S. Barrett, J. B. Newkirk and C. O. Ruud), Vol. 19, pp. 253–265. Kendahl/Hunt, Dubuque, IA.

Koschmieder H. (1924) Theorie der horizontalen Sichtweite. *Beitr. Phys. frei. Atmos.* **12**, 33–53, 171–181.

Lin C. I., Baker M. and Charlson R. J. (1973) Absorption coefficient of atmospheric aerosol: a method for measurement. *Appl. Opt.* **12**, 1356–1363.

Malm W. (1979) Considerations in measurement of visibility. *J. Air Pollut. Control Ass.* **29**, 1042–1052.

Middleton W. E. K. (1958) *Vision Through the Atmosphere*. University of Toronto Press, Toronto, Ont., Canada.

Penndorf R. (1957) Tables of the refractive index for standard air and the Rayleigh scattering coefficient for the spectral region between 0.2 and 20.0 μ and their application to atmospheric optics. *J. opt. Soc. Am.* **47**, 176–182.

Perhac R. M. (1978) Sulfate regional experiment in northeastern United States: the SURE program. *Atmospheric Environment* **12**, 641–647.

Stevens R. K., Dzubay T. G., Russwurm G. and Rickel D. (1978) Sampling and analysis of atmospheric sulfate and related species. *Atmospheric Environment* **12**, 55–68.

Tombach I. (1978) A critical review of methods for defining visual range in pristine and near pristine areas. Paper number 78-43.2 presented at the 71st annual meeting of the Air Pollution Control Association in Houston, TX, 25–30 June.

Tombach I. and Allard D. (1980) Intercomparison of visibility measurement methods. *J. Air Pollut. Control Ass.* **30**, 134–142.

Trijonis J. and Yuan K. (1978) Visibility in the Northeast. U.S. Environmental Protection Agency Report EPA 600/3-78-075, Research Triangle Park, NC 27111, U.S.A.

Trijonis J. (1979) Visibility in the Southwest: an exploration of the historical data base. *Atmospheric Environment* **13**, 833–843.

Waggoner A. P. and Charlson R. J. (1976) Measurements of aerosol optical parameters. In *Fine Particles* (Edited by B. Y. H. Liu), pp. 511–533. Academic Press, New York, NY.

Waggoner A. P. and Weiss R. E. (1980) Comparison of fine particle mass concentration and light scattering extinction in ambient aerosol. *Atmospheric Environment* **14**, 623–626.

Weiss R. E., Waggoner A. P., Charlson R. J., Thorsell D. L., Hall J. S. and Riley L. A. (1979) Studies of the optical, physical and chemical properties of light absorbing aerosols. In *Proceedings Carbonaceous Particles in the Atmosphere* (Edited by T. Novakov), pp. 257–262, Lawrence Berkeley Laboratory Report LBL-9037, CONF-7803101, UC-11, Berkeley, CA.

Willeke K. and Brockmann J. E. (1977) Extinction coefficients for multimodal atmospheric particle size distributions. *Atmospheric Environment* **11**, 995–999.